Accuracy of ice concentration derived from ERS-1 SAR images during the late melt period in the Arctic

by J. Askne, L.M.H. Ulander, and D. Birkeland

Department of Radio and Space Science
Chalmers University of Technology

ABSTRACT

Accurate ice concentration values are important for climate modelling and should also be useful for improving the accuracy of passive radiometry. Ice concentration can be determined from SAR images with an accuracy of a few percent using the global ice concentration algorithm during the advanced melt period when only old ice and open water areas are present. With the high resolution of the SAR, a large number of sample areas can be obtained from a 100 x 100 km^2 SAR scene and used to estimate the concentrations of old ice and open water. If systematic changes take place over the SAR scene, the area over which the ice concentration is to be determined has to be reduced, but not so much that local properties dominate. Melt ponds are mainly responsible for the large scale variability, and the melt pond concentration can vary considerably. On scales larger than 10 km and smaller than 100 km, representative measurements should, however, be obtained.

Key words: Arctic, Ice concentration, Melt period, ERS-1, SAR

1. INTRODUCTION

Models of global climate change indicate global warming due to increase of greenhouse gases and observational results obtained from passive microwave observations using SMMR [1] are in line with models. However the changes are small (decreasing ice cover of the Arctic with $2.1 \pm 0.9\%$ during the 8.8-year) and accurate methods are necessary to monitor changes of the Arctic ice as the warming effect is likely to be most pronounced in this area, [2].

Passive microwave radiometry from satellite has regularly been used to determine ice properties in the Arctic. One of the important parameters is the ice concentration, as the heat exchange from open water areas is considerably greater than from ice covered areas. The overall accuracy using passive microwave radiometry has been estimated from Landsat-SSMI comparisons which show a standard deviation of $\pm$ 7% [3]. Under melt conditions the offset can be as large as 10%. The high-resolution (30 m x 30 m) synthetic aperture radar (SAR) onboard the ERS-1 has a potential for highly accurate ice concentraion estimates, but oly parts of the Arctic is regularly covered. We therefore anticipate that the ERS-1 SAR will provide useful results which may be used to improve the microwave radiometer estimates.

In this paper we will concentrate on the advanced melt period, typically August when the remaining snow is very wet. The observational results are obtained in conjunction with the advanced melt period of ARCTIC-91, the International Arctic Ocean Expedition 1991, which included a program for remote sensing and sea ice based on ERS-1 [4] onboard the Swedish icebreaker Oden. The objectives of this program were to measure ice properties of importance for climate research and to explore the use of the ERS-1 SAR for measurements of Arctic sea ice.

2. ICE CONCENTRATION ALGORITHMS

Methods for ice concentration analysis were proposed by Askne and Ulander, [4]. The determination of ice concentration is based on the different radar backscatter of open water and ice. During the late melt period we have old ice and open water making the image classification simple. However the signature of old ice is influenced by melt ponding, temperature effects, etc. and the ocean signature is influenced by the wind structure, melt water, up welling, etc. and can be quite complex, in particular in the marginal ice zone.

A straightforward method to determine the ice concentration could have been to use a thresholding technique. If so, the incidence angle dependence of the backscatter signatures of ice and water are different, which makes it necessary to determine a range dependent threshold. The weakness of this method, however, is the definition of the threshold value. For relatively high ice concentrations image histograms often show no peaks even after speckle reducing filtering. Due to the uncertainties in the definitions and choice of the thresholding values, the errors associated with the method are impossible to estimate accurately, see also discussion in [5].

3. THE GLOBAL ICE CONCENTRATION ALGORITHM

The so called global ice concentration algorithm [4] is similar to the passive radiometry method using "tie point"-values, typical values for old ice (including melt ponds etc.) and water. The mean pixel intensity over certain sample areas are related to these tie point values. By pixel intensity we mean

$$I = DN^2 - DN_n^2 \quad (1)$$

where DN_n^2 is the digital pixel value squared and DNn is the noise value. Mean pixel intensities for ice and water are denoted I_i and I_w. The mean pixel intensity, the expectation value, is obtained by

$$E\{I\} = C(I)I_i + [1-C(I)]I_w \quad (2)$$

or for the spatial average of the ice concentration, <C>,

$$\langle C\rangle = \frac{\langle E\{I\}\rangle - I_w}{I_i - I_w} \quad (3)$$

The speckle problem of SAR images is eliminated by taking a mean value over a sufficiently large area.

4. BASIC ASSUMPTIONS AND ACCURACY

The "tie-points" I_i and I_w are determined by sampling typical areas over the image. The average pixel intensity in the areas is assumed to have a normal distribution (in dB) caused by texture, in the ice case mainly determined by the melt ponding, surface roughness and wetness. The texture of the water surface is controlled by the turbulence of the wind as well as melt water from the ice.

We now assume there are no systematic effects on the radar backscatter coefficient over the image beside the incidence angle dependence θ. This is approximated by a linear dependence between I [in dB-units] and θ, cf Fig. 1. The straight line obtained by regression technique (the j:th sample area located at θ_j) is used as the best estimate of the old ice and water tie points.

The mean incidence angle of the N sample area measurements distributed over the entire image, cf. [6], is defined by

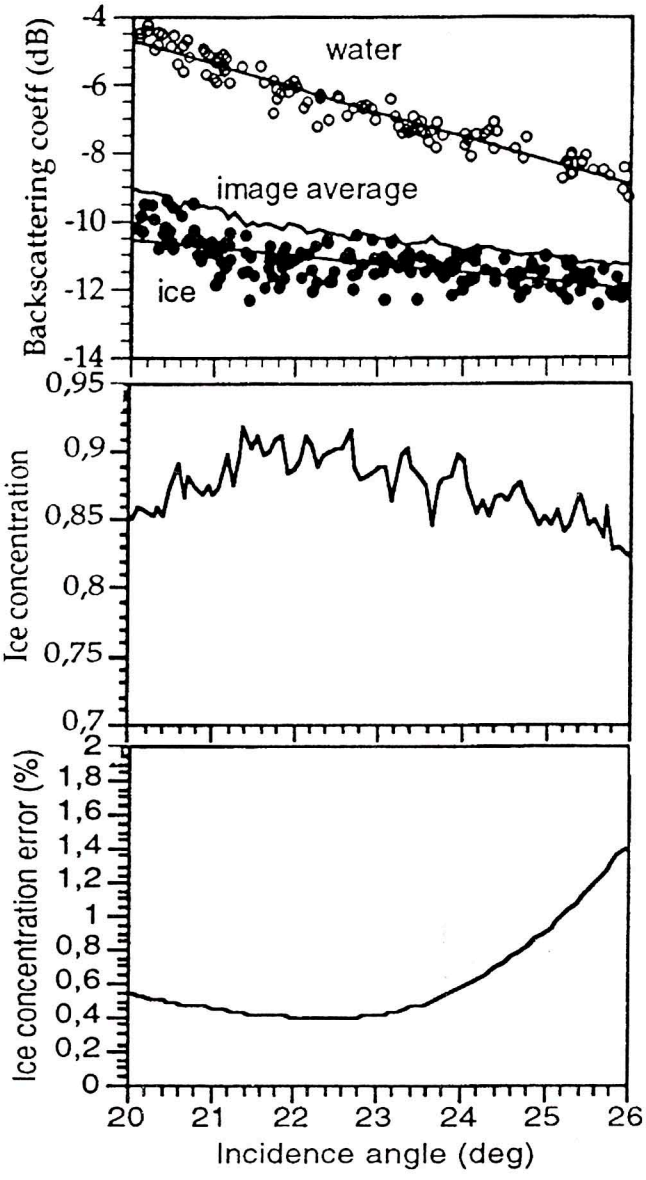

Fig. 1 - Illustrating backscattering coefficients for ice and open water, ice concentration values as averaged over azimuth and the estimated error (values derived from ERS-1 FD images on 20 August 1991 centred around 83.9 N, 28.3 E). Note that the backscatter coefficient values are based on calibration using two 1.7 m large radar reflectors within the scene. The values should be decreased by 1.6 dB to agree with the D-PAF values.

$$\bar{\theta} = \frac{1}{N} \sum_{1}^{N} \theta_i \tag{4}$$

The error of I_i and I_w for a particular incidence angle is now determined for each one by an expression of the form:

$$\Delta I^2(\theta) = \Delta I^2_{text} \left[\frac{1}{N} + \frac{(\theta - \bar{\theta})^2}{\sum_{1}^{N} (\theta_i - \bar{\theta})^2} \right] \tag{5}$$

i.e. partly determined by the texture in the form of ΔI^2_{text}, and partly by the number of sample areas, N, and their range distribution. Fig. 1a illustrates sample areas, regression line representing tie points and mean pixel intensity averaged along track over the SAR image acquired on 20 August 1991. Fig. 1b and c illustrates $C(\theta)$, and the result of the error analysis of $C(\theta)$ using (5). In this case we have identified 177 sample areas for old ice with a standard deviation (texture) around the straight line corresponding to ice in Fig. 1a of 0.46 dB and similarly 110 areas of open water with a standard deviation around the straight line corresponding to water of 0.31 dB. We see that an accuracy of the order of 1% in ice concentration is obtained. This is dependent on the number of sample areas and incidence angle as seen from (5), and on the ice concentration and contrast between ice and water as seen from the error analysis of (3).

A large ice concentration means that the ice texture dominates the error. In this case the full resolution of ERS-1 is also important to identify open water areas. In five images from 17 to 20 August open water areas have varied in mean size between 200 and 2000 pixels. A resolution change from 25 to 100 m would mean a problem to uniquely identify such areas. For lower ice concentrations on the other hand an accurate value of open water is rather important. However, in this paper we primarily study effects on the accuracy due to the ice texture, in which case the effect of melt ponds is an important factor. Note that as long as the sample area values for ice are obtained by averaging over ice floes without excluding possible melt ponds, the ice concentration value obtained is the value for ice including melt ponds.

5. ICE CONCENTRATION ACCURACY ON DIFFERENT SCALES

The radar backscatter of ice depends on properties like surface roughness and volume scattering. During summer melt, most of the backscattered energy comes from the surface, since liquid water and brine masks the underlying surface. Open melt ponds will contribute significantly due to the wind-roughened water surface. The regression technique described above assumes a large number of independent sample areas with the assumed Gaussian distribution. The regression line determines the tie points which together with (3) gives the ice concentration. Ice concentration may be computed for smaller areas than the regression line was based on, but this is only meaningful if the area is much larger than the typical scale of the old ice backscatter fluctuations. Our experience is that the present algorithms work satisfactorily for determining ice concentration maps in 10 x 10 km^2 areas but not in 1 x 1 km^2 areas.

In order to use the full accuracy of the global method, sample areas are selected for the entire image. This is only correct as long as no systematic changes of the scattering properties are taking place. Obvious reasons for systematic changes are related to temperature and wind changes. Information on such changes can be obtained from numerical forecasts.

Melt ponds

Variability in coverage of melt ponds over the image will affect the accuracy of the ice concentration estimate. So far we have not found or analysed any case where we have clear indications of systematic variations of the melt pond coverage, although we have found a variability over a relatively limited scale. We have also studied how melt ponds affect the radar backscatter.

During ARCTIC-91 we made visual observations of melt-ponding from the bridge of Oden reported every hour from 18 - 22 August. During this period Oden moves from 81N 20 E to 84 N 37 E and the mean reported melt pond concentration is 22 % (accuracy is estimated to be not better than ± 10 %) along this route with a variation from 5 to 40% with two outliers at 60 %. A video mosaic over a 10 x 0,7 km large area and with a resolution of 1.8 m (courtesy Björn Olaf Johannessen) was used to identify melt ponds at an area centred around 84.24N 33.28 E on 20 August (see Fig. 2). The melt pond concentration varied between 12 and 31 %, which is in line with the bridge observations. We conclude that over a distance larger than tenths of km we can expect melt pond coverage variations over the values reported for much larger areas. Consequently we should not use sample areas spread over the image to determine the local ice concentration accuracy but rather use a new set of sample areas. When the number of sample areas, N, are severely limited we approach an accuracy determined by ΔI^2_{text} according to Eq. (5).

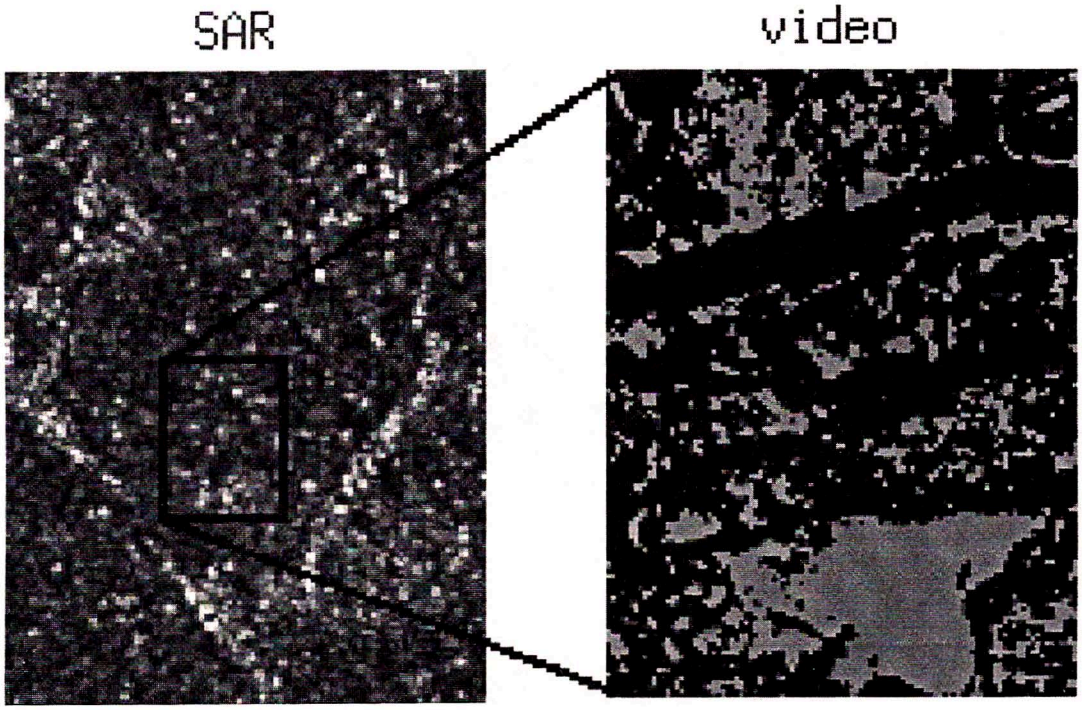

Fig. 2 - SAR and video image compared for melt pond characterisation (video courtesy Björn Olaf Johannessen)

The effect of melt ponds on the radar backscatter

The video was compared with an ERS-1 fast delivery (FD) image acquired at 13:28:59. The temperature at this time is approximately +0,4°C and the melt ponds are not frozen. The backscattering coefficient of old ice including melt ponds is plotted in Fig. 3 versus the melt pond concentration as derived from the video mosaic divided into eight areas with a size of approximately 500x500 m. As seen from the figure the melt pond concentration varies between 12 and 31%. Large melt ponds have the same characteristics as open leads and assuming the backscattering coefficient is an area average of open water (-7.0 dB at θ=24.4°) caused by the melt ponds and bare ice areas (estimated to -13.5 dB) in between, the straight line in intensity is obtained. Small melt ponds may not have the same signature as open water as the wind fetch is limited, the melt pond depth may be limited or the melt pond is shadowed by surrounding ice blocks. A classification of the melt ponds by size is therefore also included, see Table 1. The size of the melt ponds is related to the SAR FD resolution. By small melt ponds we mean smaller than one resolution cell, by medium approximately one resolution cell; by large a few resolution cells; and by giant several resolution cells. From Fig. 4 and Table 1 we conclude that in order to obtain the total backscattering coefficient to be a detectable linear mix between ice (-13.5 dB) and open water (- 7.0 dB) we must have some large or giant melt ponds within the area.

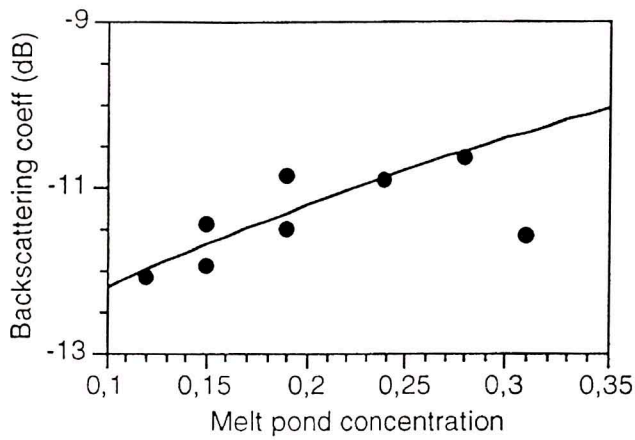

Fig. 3 - The backscattering coefficient of old ice including melt ponds versus the melt pond concentration as derived from the video mosaic. The values are based on eight areas with a size of approximately 500x500 m.

Table 1 - Classification of the melt ponds by size in relation to SAR resolution.

mpc (%)	σ° (dB)	SMALL	MEDIUM	LARGE	GIANT
12	-12.07	•	•	(•)	
15	-11.92	•	•		
15	-11.44	•	•	(•)	
19	-11.47	•	•	(•)	
19	-10.84	•	•	•	
24	-10.90	•	•	•	
28	-10.63	•	•		
31	-11.56	•	•		

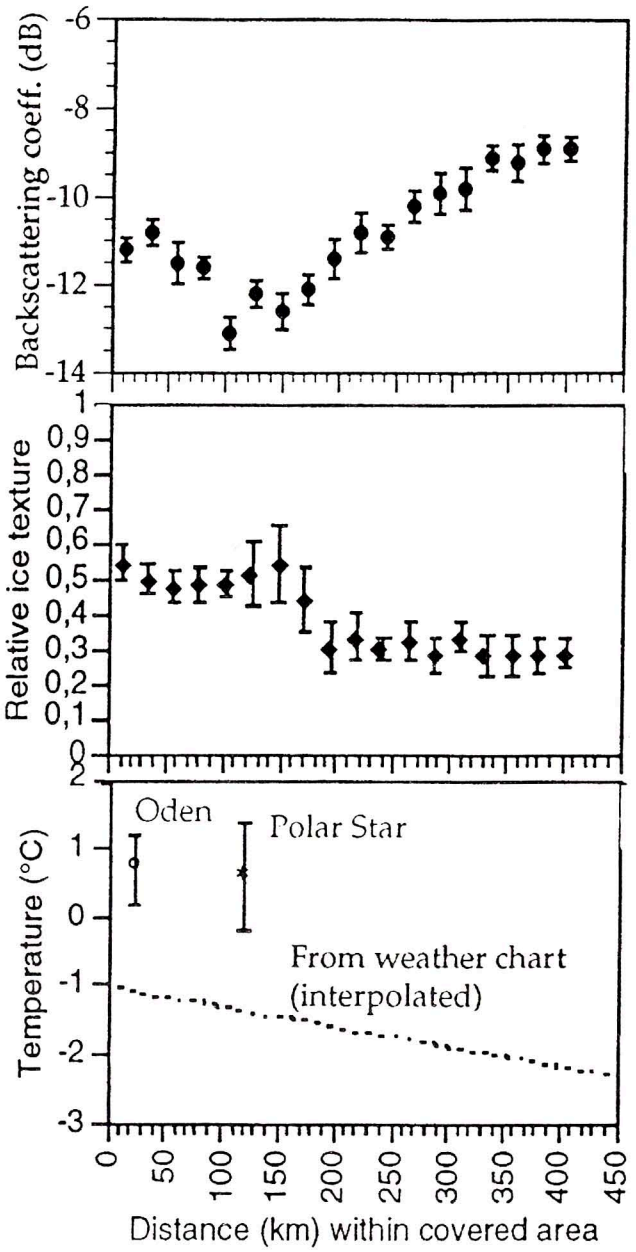

Fig. 4 - The backscatter coefficient of old ice over an area where temperatures change from above to below 0°C. Incidence angle between 21.5° and 23°.

The discussion above leads us to conclude that the old ice signature should be affected by the melt pond concentration, α, according to

$$I_I = (1 - \alpha)I_{bI} + \alpha I_w \qquad (6)$$

where I_{bI} stands for bare ice and I_w stands for the water signature which is dependent on the wind speed and direction. The expression puts demands on not only the backscatter coefficient but also the slopes with incidence angle. Studying the values from 20 August in Fig. 1 and using the estimate of -13.5 dB for bare ice (obtained from large floe with no visible melt ponds and referred to 24.4° by scattering models, [6,7]) we obtain that α = 20 %. The obtained melt pond concentration should be smaller than the true one due to the limited effect of wind on melt ponds. Backscatter values derived from FD images during the early part of the commissioning phase are somewhat uncertain. We have therefore concentrated on 20 August when radar reflectors were used in the field for calibration. Consequently it is too little data to conclude anything about the melt ponds effect on the radar cross section. It would also be of value to compare the results obtained by SAR with those obtained by SSM/I over the same area. It has been reported [8] that there are differences between SAR and SSM/I which could be due to the melt ponds which are detected by SSM/I as open water.

Systematic changes of meteorological conditions.

A decrease in temperature below freezing reduces melt pond coverage, surface wetness and brine volume. Meanwhile volume scattering due to air bubbles is expected to increase. This is illustrated in Fig. 4, where the backscatter coefficient of old ice has a minimum when the temperature can be expected to be very close to 0°C and then increases for lower temperatures. The changing temperature also shows up in the texture (standard variation over mean value) which is high for air temperatures above 0°C, probably due to the melt pond effect and uneven melting of the snow surface. This situation has been studied in a recent paper, [9].

Complex effects can also be caused by a change of wind speed and direction. The effect of wind on the capillary waves can also change due to viscosity changes caused by melt water run-off from the ice. Such effects have probably been identified [6] in one of the images from ARCTIC-91. The effects of wind have not yet been analysed in detail.

6. CONCLUSION

It is found that ice concentration can often be determined from SAR images with an accuracy of a few percent using the global ice concentration algorithm and a large number of sample areas from a 100x100 km^2 SAR image. If systematic changes of the tie point values take place over the SAR scene, the studied image size has to be reduced accordingly. For smaller areas the varying melt pond concentration has to be taken into account. The melt pond concentration varied in the area studied between 5 and

40% and according to registrations onboard Oden we may expect a full set of such variations over areas smaller than 100 km and larger than 10 km. Systematic temperature effects are obtained when the temperature varies around 0°C and wind changes may also occur over larger areas. Such variations limit the upper size of the image used to determine the set of sample values, while melt pond concentration limits the lower size. The size in between agrees with the resolution of passive microwave radiometry.

Accurate ice concentration values are important for climate modelling and should also be useful for improving the accuracy of passive radiometry estimates. The melt pond concentration is also a parameter of great interest for climate modelling, and we see some possibilities to study the melt pond concentration by using the back scatter coefficient, but these results are preliminary and should be further analysed.

ACKNOWLEDGEMENT

The support from the Swedish Space Agency is gratefully acknowledged.

Björn Olaf Johannessen, SINTEF, NHL, Trondheim, is acknowledged for the video mosaic as part of the Sea Ice and Remote Sensing Program onboard Oden, and Dagfinn Birkeland for help in the calculation of ice concentration properties from the SAR images.

REFERENCES

[1] Gloersen P. & Campbell W.J., 1991, "Recent Variations in Arctic and Antarctic Sea-Ice Cover", Nature, vol. 352, pp 33-36.

[2] Stouffer R.J., Manabe S. & Bryan K., 1989 "Inter hemispheric Asymmetry in Climate Response to a Gradual Increase of Atmospheric CO_2" Nature, vol. 342, pp 660-662.

[3] Steffen K. & Schweiger A., 1991. "DMSP-SSMI NASA Team Algorithm for Sea Ice Concentration Retrieval: Comparison with Landsat Satellite Imagery", J. Geophys. Res. vol 96, pp 21971-21987.

[4] Askne J. & Ulander L.M.H., 1992, "Remote Sensing of Arctic Sea Ice using the ERS-1 SAR", Proceedings European ISY symposium, pp 129-133.

[5] Askne J., Ulander L.M.H., Carlström A., Sun Y. & Birkeland D., Validation of ERS-1 SAR Measurements of Sea Ice during ARCTIC-91, Proceedings First ERS-1 Symposium, Cannes, France, 4 - 6 Nov. 1992, ESA SP-359, pp 289-294.

[6] Askne J., Ulander L.M.H., Carlström A. & Sun Y., 1993, "Remote Sensing of Arctic Sea Ice by ERS-1: A Status Report", in P. Winkler, editor, Remote Sensing for Monitoring the Changing Environment of Europe, pp 43-51, A.A. Balkema.

[7] Carlströma. & Ulander L.M.H., 1993, "C-band Backscatter Signatures of Old Sea Ice in the Central Arctic during Freeze up", IEEE Trans. Geoscience and Remote Sensing, vol 31, 819-829.

[8] Comiso J.C. & Kwok R., "Summer Arctic Ice Concentrations and Characteristics from SAR and SSM/I data", Proceedings First ERS-1 Symposium, Cannes, France, 4 - 6 Nov. 1992, ESA SP-359, pp 367-372.

[9] Askne J., Ulander L.M.H. & Birkeland D., 1993, "ERS-1 SAR Analysis of Arctic Ice Concentration during the Melt Season, Proceedings of IGARSS'93 held in Tokyo, 18-21 August, 1993, IEEE 93CH3294-6, pp. 431-433.